the FEBS Journal

Determination of the metal ion dependence and substrate specificity of a hydratase involved in the degradation pathway of biphenyl/chlorobiphenyl

Pan Wang and Stephen Y. K. Seah

Department of Microbiology, University of Guelph, Ontario, Canada

Keywords
aromatics; hydratase; 2-hydroxypent-2,4-dienoate; metal cofactor; substrate specificity

Correspondence
S. Y. K. Seah, Department of Microbiology, University of Guelph, Guelph, Ontario, Canada, N1G 2W1
Fax: +1 519 837 1802
Tel: +1 519 824 4120 Ext. 56750
E-mail: sseah@uoguelph.ca

(Received 22 October 2004, revised 9 December 2004, accepted 15 December 2004)

doi:10.1111/j.1742-4658.2004.04530.x

BphH is a divalent metal ion-dependent hydratase that catalyzes the formation of 2-keto-4-hydroxypentanoate from 2-hydroxypent-2,4-dienoate (HPDA). This reaction lies on the catabolic pathway of numerous aromatics, including the significant environmental pollutant, polychlorinated biphenyls (PCBs). BphH from the PCB degrading bacterium, *Burkholderia xenoverans* LB400, was overexpressed and purified to homogeneity. Atomic absorption spectroscopy and Scatchard analysis reveal that only one divalent metal ion is bound to each enzyme subunit. The enzyme exhibits the highest activity when Mg^{2+} was used as cofactor. Other divalent cations activate the enzyme in the following order of effectiveness: $Mg^{2+} > Mn^{2+} > Co^{2+} > Zn^{2+} > Ca^{2+}$. This differs from the metal activation profile of the homologous hydratase, MhpD. UV-visible spectroscopy of the Co^{2+}–BphH complex indicates that the divalent metal ion is hexa-coordinated in the enzyme. The nature of the metal ion affected only the k_{cat} and not the K_m values in the BphH hydration of HPDA, suggesting that cation has a catalytic rather than just a substrate binding role. BphH is able to transform alternative substrates substituted with methyl- and chlorine groups at the 5-position of HPDA. The specificity constants (k_{cat}/K_m) for 5-methyl and 5-chloro substrates are, however, lowered by eight- and 67-fold compared with the unsubstituted substrate. Significantly, k_{cat} for the chloro-substituted substrate is eightfold lower compared with the methyl-substituted substrate, showing that electron withdrawing substituent at the 5-position of the substrate has a negative influence on enzyme catalysis.

Microbial degradation of aromatic compounds is important for maintaining the global carbon cycle and also for the bioremediation of man-made aromatic compounds, released in the environment due to industrial activities. Diverse aromatic compounds, including biphenyl [1], xylenes [2] and 3-(3-hydroxyphenyl)propionate [3], can be degraded via the *meta*-cleavage pathway, where the respective compounds is first converted to a catechol. Subsequent enzymatic transformation of the cleaved catechol leads to the formation of the common intermediate 2-hydroxypent-2,4-dienoate (HPDA). This intermediate can then be converted to pyruvate and acetyl CoA by three further steps in the pathway. The first of these three steps is catalyzed by a divalent cation-dependent hydratase (EC 4.2.1.80) that transforms HPDA to 2-hydroxy-4-ketopentanoate (Fig. 1).

Among the *meta*-cleavage pathway enzymes, the last three enzymes, responsible for the final formation of tricarboxylic acid cycle intermediates, are comparatively

Abbreviations
BphH, MhpD, XylJ, HPDA hydratases; HPDA, 2-hydroxypent-2,4-dienoate; HODA, 2-hydroxy-6-oxohexa-2,4-dienoate; PCBs, polychlorinated biphenyls; TodF, 2-hydroxy-6-oxohepta-2,4-dienoate hydrolase; XylE, catechol dioxygenase.

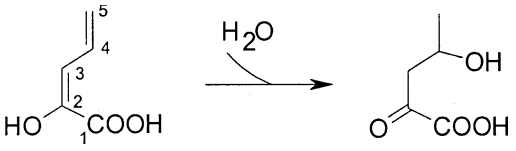

Fig. 1. Reaction catalyzed by HPDA hydratase. Carbon numbering of the HPDA substrate is indicated.

less well studied. For example, there have been no systematic substrate specificity studies of HPDA hydratases, although HPDAs substituted with methyl or chlorine groups can arise from the transformation of certain aromatics such as *p*-xylene or polychlorinated biphenyls (PCBs) [4]. In addition, the role of the essential divalent metal ion in the hydratase has not been resolved.

Mechanistic studies using XylJ, the HPDA hydratase in the xylene degradation pathway of *Pseudomonas putida* pWW0, show that the enzyme catalyzes deuterium exchange of the C3 and C5 protons of the dienol substrate [5,6]. The related MhpD (47% amino acid sequence identity to XylJ) is strongly inhibited by oxalate [7]. This led to the proposed mechanism whereby the dienol substrate is first tautomerized to a *cis*-keto anion intermediate, which then undergoes the Michael addition of water. The hypothesis that the keto intermediate has a *cis* rather than *trans* geometry is based on the observation that the enzyme cannot hydrate the *trans*-keto form of HPDA that is spontaneously formed in aqueous solution [7,8]. The function of the metal ion in the hydratase is not clear in these studies. MhpD was not inhibited by crotonyl hydroxamate, suggesting that substrate does not bind to the metal ion in a bidentate manner i.e. through both the C1-carboxyl and C2-carbonyl oxygens [7]. Based on mechanistic consideration, interaction of the divalent cation with the C2-carbonyl oxygen is expected to stabilize the enolate anion transition state. Interaction with only the C1-carboxyl, on the other hand, may aid in substrate binding. The number of cations bound per enzyme active site has not been determined in any HPDA hydratase and it is therefore unclear if the metal ion(s) has one or both of the proposed functions.

Here we report the overexpression and purification of recombinant BphH (53 and 71% amino acid sequence similarity to MhpD and XylJ, respectively), a HPDA hydratase from the polychlorinated biphenyls (PCBs) degradation pathway in *Burkholderia xenovorans* LB400 [9,10]. The availability of large quantities of monofunctional enzyme allows us to determine, for the first time, the number of metal ions bound to each hydratase by atomic absorption spectroscopy. We measured the dissociation constants of Mg^{2+} and Mn^{2+} and the influence of each metal cofactor on the kinetic parameters for HPDA hydration. We also generate and test the specificity of the enzyme towards alternative substrates with chlorine and methyl functional groups at the 5-position. Together, these results provide insight regarding the mechanism, the substrate binding site and the role of the metal cofactor in the enzyme.

Results

Cloning, expression and purification of BphH

The *bphH* gene was inserted into the expression vectors pT7-7 [11], pEMBL18 [12] and pVLT31 [13], which contain the T7, *lac* and *tac* promoters, respectively. The pT7-7 and pEMBL18 constructs were transformed into *Escherichia coli* BL21 (λDE3) and *E. coli* DH5α, respectively. Attempts to produce BphH in these *E. coli* strains, at 37 °C and 18 °C, led to insoluble inclusion bodies formation. BphH can, however, be expressed in soluble form from *Pseudomonas putida* KT2442 using the pVLT31 construct. The enzyme constitutes about 20% of the soluble proteins in this bacterium as estimated from SDS/PAGE. Overproduced BphH was purified by anion exchange, hydrophobic interaction and gel filtration chromatography to about 95% homogeneity with a yield of 38.8 mg of enzyme per liter of cultured cells (Table 1, Fig. 2).

General properties of BphH

The subunit molecular mass of BphH, as determined by SDS/PAGE, is 27 ± 1 kDa. This is in agreement with the predicted molecular mass of 27.3 kDa, based on its amino acid sequence. By gel filtration, the native molecular mass of BphH is 221 ± 25 kDa, suggesting

Table 1. Purification of BphH. BphH was purified from 1 L of cells. Assays contain 0.2 mM HPDA and 3 mM $MgSO_4$ in 100 mM potassium phosphate buffer, pH 6.0. Substrate utilization was monitored at 265 nm using the determined extinction coefficient of 15.85 ± 0.29 $mM^{-1}·cm^{-1}$ for HPDA. One unit is the enzyme required to transform 1 μmol of HPDA substrate in 1 min.

Step	Protein (mg)	Activity (U)	Specific activity ($U·mg^{-1}$)	Recovery (%)	Purification (*n*-fold)
Cell extract	508	4.16×10^4	81.9	100	1.00
Source™ 15Q	81.7	2.44×10^4	306	59.0	3.74
PhenylSepharose™	44.9	2.37×10^4	528	57.0	6.45
Superdex™ 200	38.8	2.07×10^4	533	49.7	6.51

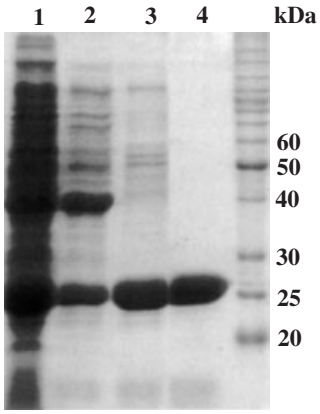

Fig. 2. Coomassie-blue stained SDS/PAGE of purified BphH. The gel was loaded with samples of BphH from crude extract (lane 1); preparation after anion exchange (lane 2); preparation after hydrophobic column chromatography (lane 3), preparation after gel filtration (lane 4). The molecular mass of the proteins in the standard (lane 5) are indicated beside the gel.

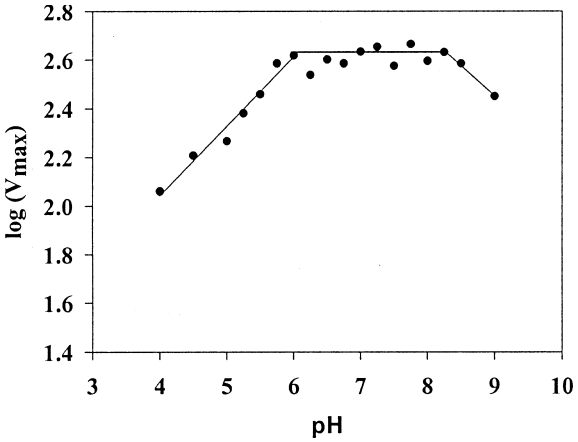

Fig. 4. pH dependence of BphH activity. Assays were performed as described in Experimental procedures. Spontaneous substrate tautomerization rate is too rapid at pH above 9.0 to reliably measure the enzyme catalyzed transformation.

that the enzyme adopts an octameric quartenary structure, assuming that it is globular.

The enzyme has no activity when divalent cations are excluded from the enzyme assay mixture. Therefore the native divalent cation, essential for the enzyme's activity, is not tightly bound to the enzyme and is lost during chromatographic purification of BphH. The apoenzyme can, however, be reconstituted with Mg^{2+} *in vitro* and the specific activity of the purified enzyme in the presence of saturating amounts of Mg^{2+} is 533 $U{\cdot}mg^{-1}$.

The relative specific activity of BphH was tested with different divalent cations (Fig. 3). $CuCl_2$ and $CuSO_4$ did not activate BphH activity. Activity of the enzyme is highest with Mg^{2+} followed by Mn^{2+}. This is in contrast to the homologous hydratase, MhpD, where it is reported that the enzyme has the highest activity with Mn^{2+} as cofactor [7]. Chloride or sulfate salts of the respective divalent cations appear to have no significant effect on the specific activity of the BphH.

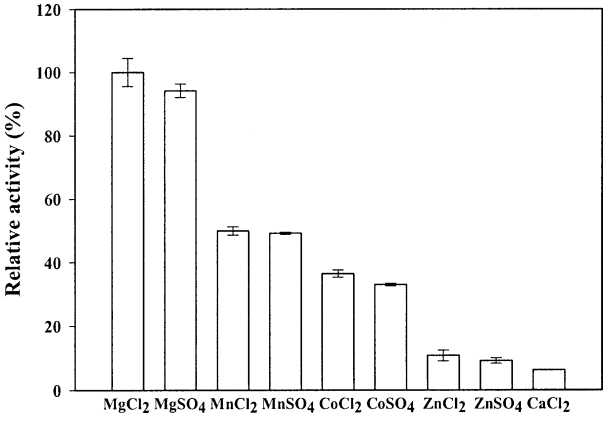

Fig. 3. Relative activity of BphH with various divalent metal salts. Activity obtained with $MgCl_2$ is taken as 100%. Assays were performed with 0.7 $\mu g{\cdot}mL^{-1}$ BphH, 0.2 mM of HPDA and 1 mM of the respective divalent metal ions in 100 mM phosphate buffer, pH 6.0.

The activity of BphH-Mg^{2+} was determined at pH values between 4.0 and 9.0, using constant ionic strength pH buffers (Fig. 4). The enzyme has relatively constant activity between pH 6.0 and 8.0, but activity rapidly decreases below and above this pH range. In contrast to the metal activation profile, the pH-rate profile of BphH is similar to MhpD, suggesting that both enzymes utilize similar residues with p*K*a values of 6.0 and 8.0 for catalysis.

Number of metal ion bound per enzyme and determination of coordination number

The equilibrium concentration of Mg^{2+} bound to BphH was determined by atomic absorption spectroscopy. A maximum of 1.12 ± 0.09 mole of Mg^{2+} was bound per mole of enzyme, suggesting that only a single metal ion is present per enzyme subunit.

To determine the metal coordination number, UV-visible spectroscopy was performed on the Co^{2+}–BphH complex. No strong absorbance features between 500 nm to 700 nm was detected which is characteristic of symmetry forbidden d–d transition and indicative of an octahedral rather than a tetrahedral metal coordination [14].

Metal ions affinity and kinetic constants for HPDA

Binding affinities of BphH towards Mg^{2+} and Mn^{2+} were determined by steady-state kinetic analysis of the metal-dependent hydration of HPDA. The data can be fitted to a single straight line in a Scatchard plot consistent with the presence of only one metal ion in each enzyme subunit (Fig. 5). From the Scatchard plot, the dissociation constant of Mn^{2+} is determined to be 3.02×10^{-6} M, which is two orders of magnitudes lower than for Mg^{2+} ($K_d = 5.74 \times 10^{-4}$ M). Interestingly, even though the enzyme's affinity for Mg^{2+} is weak, BphH has the highest specific activity when saturated with this metal ion.

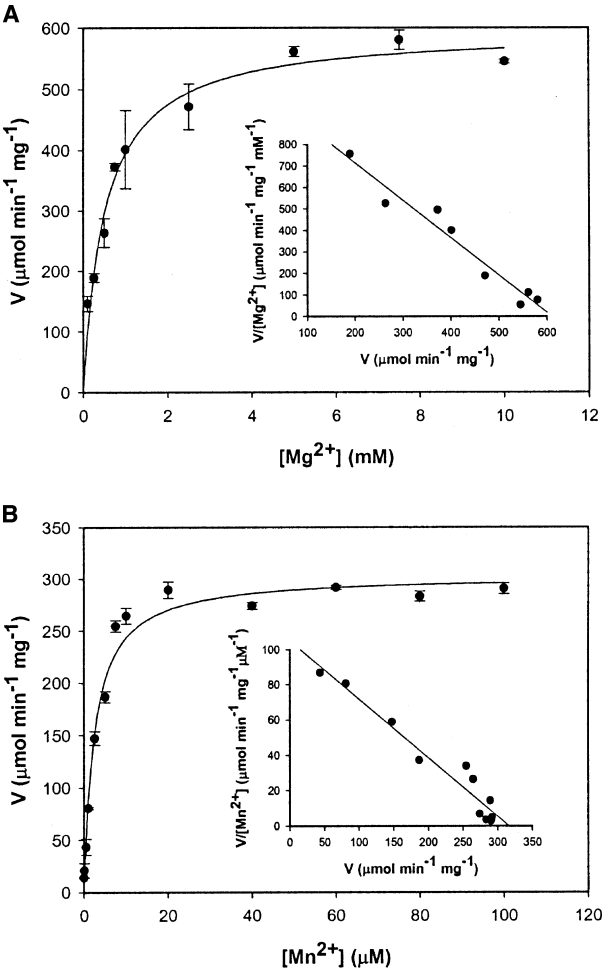

Fig. 5. Dependence of BphH activity in varying concentrations of (A) Mg^{2+} and (B) Mn^{2+}. Assays were performed with 100 mM phosphate buffer, pH 6.0 containing 0.2 mM HPDA and 0.35 μg·mL^{-1} BphH. The same data are represented as a Scatchard plot (inset).

Table 2. Kinetic parameters for HPDA hydration catalyzed by BphH saturated with Mg^{2+} or Mn^{2+}. Assays were performed at 25 °C and they contained 3 mM divalent cation and 0.35 μg·mL^{-1} BphH in 100 mM potassium phosphate buffer, pH 6.0.

Metal cofactor	K_m (μM) HPDA	k_{cat} (s^{-1})	k_{cat}/K_m ($M^{-1}·s^{-1} \times 10^{-6}$)
$MgSO_4$	31.7 ± 1.3	361 ± 6	11.4 ± 0.6
$MnSO_4$	38.6 ± 1.4	215 ± 4	5.6 ± 0.3

The influence of the two metal ions on the kinetic parameters for HPDA hydration by BphH is shown in Table 2. The K_m values were similar with either metal cofactor. On the other hand, the k_{cat} value is higher by 1.7-fold with Mg^{2+}. This suggests that the nature of the metal ion has a predominant influence on catalysis rather than substrate binding.

Substrate specificity of BphH

Substrate specificity of Mg^{2+} saturated BphH was determined by steady state kinetic analysis. As HPDAs are unavailable commercially, the substrates were generated enzymatically from 4-methylcatechol and 4-chlorocatechol using the purified catechol dioxygenase, XylE [15] and 2-hydroxy-6-oxohepta-2,4-dienoate hydrolase, TodF [16].

The BphH activity data for 5-methyl-HPDA and 5-chloro-HPDA can be fitted to classical Michealis–Menten equation and the kinetic parameters are summarized in Table 3. Specificity constants for 5-methyl-HPDA and 5-Cl-HPDA are lowered eight- and 67-fold, respectively, in comparison to the unsubstituted HPDA (Table 2). Interestingly, the lower specificity of the enzyme towards the 5-substituted substrates is mainly attributed to low turnover numbers (k_{cat}), as the Michealis constants (K_m) are increased by only about 1.3-fold. Thus, BphH active site can

Table 3. Specificity of BphH towards 5-substituted HPDA substrates. Assays contained 3 mM $MgSO_4$ in 100 mM potassium phosphate buffer, pH 6.0. Substrate conversion was monitored at the wavelength of maximum absorbance for each substrate, which is 276 nm for 5-methyl-HPDA and 278 nm for 5-chloro-HPDA. Extinction coefficients of 5-methyl-HPDA and 5-chloro-HPDA are determined as described in Experimental procedures and found to be 16.51 ± 0.17 $mM^{-1}·cm^{-1}$ and 13.57 ± 0.69 $mM^{-1}·cm^{-1}$, respectively.

Substrate	K_m (μM)	k_{cat} (s^{-1})	k_{cat}/K_m ($M^{-1}·s^{-1} \times 10^{-6}$)
5-Methyl-HPDA	40.8 ± 2.6	60.5 ± 1.6	1.5 ± 0.1
5-Chloro-HPDA	45.9 ± 4.5	7.7 ± 0.3	0.17 ± 0.02

accommodate the larger 5-substituted substrates. However, the presence of electron withdrawing chlorine substituent at the 5-position resulted in an eightfold lower k_{cat} value compared with the methyl substituted substrate.

Discussion

HPDA hydratase, an enzyme in the *meta*-cleavage pathway of aromatic compounds, catalyzes a hydration reaction via a proposed anion transition state. Previous studies with MhpD, suggest that this hydratase may bind two divalent cations, one interacting with the C2-carbonyl oxygen and the other to C1-carboxyl oxygens [7]. Due to insufficient amounts of purified enzyme, quantitative metal binding studies have not been performed in MhpD. Another HPDA hydratase, XylJ, on the other hand, can only be expressed as a complex with a decarboxylase (XylI), the preceding enzyme in the xylene degradation pathway [5]. The binding of divalent cations by the decarboxylase precludes metal binding studies of the hydratase in that complex.

In this study, BphH, the hydratase in the PCBs degradation pathway of *B. xenoverans* LB400, was overexpressed and purified with high yield. The enzyme is active without any associated enzymes. Using atomic absorption spectroscopy, we show that the apoenzyme binds to a single Mg^{2+} per enzyme subunit. Data from a Scatchard analysis of the metal-dependent hydration of HPDA by BphH can be fitted into a single straight line, also indicating that there is only one metal ion bound to the enzyme in the presence of substrate. UV-visible spectra of the Co^{2+}–BphH complex demonstrate that the coordination of the single metal ion in the enzyme is octahedral rather than tetrahedral.

Divalent metal ions activate BphH in the following order of effectiveness: Mg^{2+}, Mn^{2+}, Co^{2+}, Zn^{2+} and Ca^{2+}. This differs from the metal activation profile reported for MhpD, which is 1.6-fold more active with Mn^{2+} than with Mg^{2+} [7]. In addition, the affinity of MhpD for Mn^{2+} appears to be weak, requiring 10 mM excess of Mn^{2+} to achieve maximum enzyme activity. In comparison, the concentration of Mn^{2+} required for maximal BphH activity is about 20 μM. Co^{2+} and Zn^{2+} appear to activate MhpD to a similar extent, whereas activity of BphH is threefold higher with Co^{2+} than with Zn^{2+}. Despite this difference in metal activation profile, the pH dependence of the enzyme activity and the kinetic constants of HPDA hydration for each enzyme, using the respective optimum metal ion cofactor, are similar. For example, the K_m value of 41 μM and k_{cat} of 450 s^{-1} were reported for MhpD with Mn^{2+} cofactor [7], which is of the same order of magnitude as the corresponding values determined for BphH with Mg^{2+} as cofactor. Sequence divergence between the two enzymes (amino acid sequence identity between BphH and MhpD is 37%) appears therefore to affect mainly their respective metal cofactor preferences. Despite the higher dissociation constant of BphH for Mg^{2+}, this metal ion is the likely physiological cofactor for the enzyme because it is highly abundant in cells (10^{-3} M for Mg^{2+} compared with 10^{-8} M for Mn^{2+}) [14].

In order to determine the role of the divalent metal ion in the enzyme, we performed steady-state kinetic analysis of HPDA hydration by BphH-Mg^{2+} and BphH-Mn^{2+}. Mg^{2+} is smaller than Mn^{2+} by 0.11 Å and it therefore has a higher charge density [17]. However, the nature of the metal ion was observed to only affect turnover number (k_{cat}) and not the K_m of the HPDA substrate. Therefore, the metal ion has a catalytic rather than just a substrate binding role. Possible roles of the cation include the activation of water for the hydration reaction and/or the stabilization of the anion transition state. In the latter case, if the substrate coordination to the metal ion is not bidentate, interaction of the single metal ion in the active site with the substrate C2-carbonyl oxygen instead of the C1-carboxyl oxygens, will provide the optimal stabilization of the proposed enolate anion transition state. Therefore, the higher catalytic rate observed for Mg^{2+} could be due to its higher Lewis acidity compared with Mn^{2+}. However, it should be noted that in MhpD, activity with Mn^{2+} is higher than with Mg^{2+}, suggesting that other factors, such as positions of the metal ion due to differences in active site residues among members of this group of hydratases, may also have a bearing on catalytic rate.

Substrate specificity of the first four enzymes in the *meta*-cleavage pathway has been extensively studied [4,18–20]. In contrast, no comparative substrate specificity data of the last three enzymes in the pathway are available. *B. xenoverans* LB400 is a PCBs degrading bacterium and it is therefore of interest to determine if chlorinated HPDA is transformed by BphH. The K_m value for 5-chloro-HPDA is about 1.4-fold higher than the unsubstituted substrate, while k_{cat} value is lower by 47-fold. Interestingly, the Michealis constant for 5-methyl-HPDA is also similar to 5-chloro-HPDA, but the turnover number for this substrate is eightfold higher than 5-chloro-HPDA. This result demonstrates that the active site of BphH can accommodate the larger substrates, but catalytic rate is reduced when the substrate is substituted with an electron withdrawing group. Possible explanations include a rate limiting

proton donation to the enolate intermediate, due to inductive stabilization of the anion by the electron withdrawing substituent. This is in line with previous proposal of a step-wise hydration mechanism in the HPDA hydratases [7].

Microorganisms that possess the *meta*-cleavage pathways are useful for bioremediation of aromatic pollutants. The availability of an expression system for BphH reported in this work will enable future systematic study of structure–function relationships through site-directed mutagenesis. This may form the basis for protein engineering efforts to improve the enzyme and pathway for efficient degradation of a wide range of aromatic pollutants.

Experimental procedures

Chemicals

Catechol, 4-methylcatechol and 4-chlorocatechol were from Sigma-Aldrich (Oakville, Ontario, Canada). Restriction enzymes, T4 DNA ligase and *Pfx* polymerase were from Invitrogen (Burlington, Ontario, Canada) or New England Biolabs (Pickering, Ontario, Canada). All other chemicals were of analytical grade and were obtained from Sigma-Aldrich and Fisher Scientific (Nepean, Ontario, Canada).

Bacterial strains and plasmids

Strains used for DNA manipulation or protein expression included *E. coli* DH5α [21], *E. coli* BL21(λDE3) [22] and *P. putida* KT2442 [23]. Plasmids used in this work were pT7-7 [11,22], pEMBL18 [12], pET28a (Novagen, EMD, Biosciences Inc., San Diego, CA, USA) and pVLT31 [13]. *E. coli* was grown at 37 °C while *P. putida* was grown at 30 °C. Recombinant *E. coli* strains were propagated in Luria–Bertani media supplemented with the appropriate antibiotics at concentrations of 100 $\mu g \cdot mL^{-1}$ for ampicillin, 15 $\mu g \cdot mL^{-1}$ for tetracycline and 50 $\mu g \cdot mL^{-1}$ for kanamycin. Recombinant *P. putida* were grown on Luria–Bertani medium supplemented with tetracycline (15 $\mu g \cdot mL^{-1}$) and rifampicin (50 $\mu g \cdot mL^{-1}$).

DNA manipulation

DNA was purified, digested and ligated using standard protocols [24]. N-Terminal His_6-tagged TodF was constructed by inserting the previously cloned gene [25] into the *Nde*I and *Hin*dIII sites of the expression vector pET28a. The *bphH* gene was amplified by PCR using the primers with the respective sequences 5′-CCCGCATATGACCCCTGA ACTG and 5′-CCCCAAGCTTCAGTGAAAGCGCAC. *Nde*I and *Hin*dIII restriction sites are underlined. The PCR reaction contain 10 ng of template pDD5301 [10], 0.8 units of *Pfx* polymerase (Invitrogen), 20 nM amounts of each dNTP and 100 pmol of each primer in a total volume of 100 μL. The following amplification profile was followed: 94 °C for 2 min, followed by 30 cycles of 94 °C for 30 s, 50 °C for 30 s, and 68 °C for 1 min and finally 68 °C for 10 min. The amplified fragment was purified using the concert rapid PCR purification system (Life Technologies, Inc., Burlington, Ontario, Canada), digested with *Nde*I and *Hin*dIII and ligated to the same restriction sites in pT7-7. The *bphH* gene from a positive clone was sequenced at the Guelph Molecular Supercentre, University of Guelph, to ensure no PCR-induced errors. The *bphH* gene was then excised by *Xba*I and *Hin*dIII digestion and subcloned into the vectors pEMBL18 and pVLT31.

Purification of BphH

Chromatography was performed on an ÄKTA Explorer 100 (Amersham Pharmacia Biotech, Baie d'Urfé, Quebec, Canada). Buffers containing 20 mM sodium Hepes, pH 7.5, was used throughout the purification procedure unless indicated otherwise.

The cell pellet (7 g) was resuspended in buffer and disrupted by passing through French Press twice at an operating pressure of 12 000 psi. The cell debris was removed by centrifugation at 17500 ***g*** for 30 min. The clear supernatant was filtered through a 0.45 μm filter and was loaded onto a Source™ 15Q (Amersham Pharmacia Biotech) anion exchange column (2 × 13 cm), which has been equilibrated with buffer containing 0.1 M NaCl. The column was washed with a linear gradient of NaCl from 0.1 to 0.4 M over 10 column volumes. Fractions containing BphH activity were eluted at about 0.2 M NaCl. Active fractions were pooled and concentrated by ultrafiltration with a YM10 filter (Millipore, Nepean, Ontario, Canada) and was loaded onto Phenyl Sepharose™ hydrophobic interaction chromatography column (1 × 18.5 cm), which was pre-equilibrated with 20 mM sodium Hepes, pH 8.0 containing 0.1 M ammonium sulfate. The column was washed first with a two-column volume of the same buffer and then with a two-column volume linear gradient of ammonium sulfate from 0.1 to 0 M followed by five column volumes of ammonium sulfate-free buffer. Fractions containing BphH activity were eluted at ammonium sulfate-free buffer. Active fractions were pooled and concentrated to about 4 mL by ultrafiltration with a YM10 filter and then loaded onto HiLoad™ 26/60 Superdex™ 200 prep gel filtration column (Amersham Pharmacia Biotech) that had been pre-equilibrated with buffer containing 0.15 M NaCl. The column was eluted with the same buffer at a flow rate of 3 $mL \cdot min^{-1}$. Fractions containing BphH activity were pooled and concentrated as before. Purified BphH was stored frozen in aliquots at −20 °C in 20 mM sodium Hepes buffer, pH 7.5 and its activity remained stable for at least three months.

Purification of catechol 2,3-dioxygenase (XylE)

Catechol 2,3-dioxygenase (XylE) was partially purified from recombinant *E. coli* JM101 containing the plasmid pAW31 [15]. The harvested cells from 2 L culture were resuspend in cell disruption buffer containing 20 mM sodium Hepes, pH 7.5, 10% isopropanol, 2 mM dithiothreitol and passed through French press twice. After centrifugation at 20 000 ***g*** for 30 min, the supernatant was filtered with a 0.45 μm filter. The initial NaCl concentration in the crude extract was adjusted to 0.25 M and then loaded onto a Source^{TM} 15Q (Amersham Pharmacia Biotech) anion exchange column (2 × 13 cm), which has been equilibrated with buffer containing 0.25 M NaCl. The column was washed with a linear gradient of NaCl from 0.25 to 0.4 M over 10 column volumes. Fractions containing XylE activity, based on their ability to transform catechol to a yellow product, were eluted at about 0.3 M NaCl, and were pooled and concentrated by ultrafiltration with a YM10 filter. Fresh iron(II) ammonium sulfate solution was added to final concentration of 0.5 mM, and the enzyme was aliquoted and stored at −20 °C.

Purification of hydrolase TodF

The recombinant N-terminal His_6 tagged TodF was expressed in *E. coli* BL21(λDE3) and purified by Ni–NTA agarose resin according to the nondenaturing procedure recommended by the supplier (Qiagen, Inc., Mississauga, Ontario, Canada). His_6-TodF was eluted with 50 mM sodium phosphate buffer (pH 8.0) containing 300 mM NaCl and 100 mM imidazole. TodF activity was detected based on its ability to transform yellow colored 2-hydroxy-6-oxohexa-2,4-dienoate to the colorless product, HPDA. Fractions containing TodF were pooled, concentrated by ultrafiltration and washed repeatedly with 20 mM sodium Hepes, pH 7.5, to remove imidazole from the solution. The concentrated enzyme (about 5 $mg{\cdot}mL^{-1}$) was stored frozen in aliquots at −80 °C.

Preparation of HPDA and substituted HPDA and determination of extinction coefficients

HPDA and substituted HPDA were generated enzymatically from catechol, 4-methyl catechol and 4-chlorocatechol by purified XylE and TodF, in 100 mM potassium phosphate buffer, pH 6.0. Reaction was monitored by the increase in UV absorbance. When maximum UV absorbance was reached, the reaction was quenched by addition of concentrated HCl to pH 1.0. HPDA was then extracted into ethyl acetate and concentrated using negative pressure following a previously described protocol [7,26]. The 2-hydroxy-6-oxohexa-2,4-dienoate (HODA) product from XylE cleavage of 4-cholorocatechol is also purified by ethylacetate extraction and analyzed by proton NMR and COSY using a Bruker Avance 600 spectrometer (Milton, Ontario, Canada). The resultant spectra confirmed that ring-cleavage occurs between carbon 3 and 4 forming 5-chloroHODA. ^{1}H NMR (acetone-d6): 9.54 (s, 1H), 7.89 (d, 1H, $J = 11.4$Hz), 6.68 (d, 1H, $J = 11.4$Hz) p.p.m.

Extinction coefficients of HPDA and substituted HPDA were determined by adding XylE and TodF stepwise to solutions containing known amounts of catechol and determining the resulting UV absorbance. Complete cleavage of catechol by XylE and the amounts of HODAs generated were verified based on the extinction coefficients reported previously [25].

Determination of protein concentration, purity and molecular mass

Protein concentrations were determined by the Bradford assay [27] using bovine serum albumin as standards. SDS/PAGE was performed and stained with Coomassie blue according to established procedures [28]. The BenchMark^{TM} Protein Ladder (Invitrogen) containing proteins ranging from 10 to 220 kDa was used as a molecular mass marker. To determine molecular mass of BphH, gel filtration was performed on a Superdex^{TM} 200 column (Amersham Pharmacia) using 20 mM sodium Hepes buffer (pH 7.5) containing 0.15 M NaCl as equilibration and elution buffer. The standard curve consists of the following proteins (Sigma): cytochrome *c* (molecular mass = 12.4 kDa), carbonic anhydrase (molecular mass = 29.0 kDa), bovine serum albumin (molecular mass = 66.0 kDa), alcohol dehydrogenase (molecular mass = 150.0 kDa), and β-amylase (molecular mass = 200.0 kDa).

Kinetic assays and substrate specificity determination of BphH

BphH activity assay was performed by following the HPDA substrate utilization as previously described [7]. All kinetics assays were performed at least in duplicate at 25 °C using a Varian Cary 100 spectrophotometer equipped with a thermojacketed cuvette holder. One unit of enzyme represents the amount of protein that convert 1 μmol of substrate to product in 1 min.

The standard activity assay during BphH purification was performed in a total volume of 1.0 mL and contained 100 mM potassium phosphate buffer pH 6.0, 3 mM $MgSO_4$ and 0.2 mM HPDA. Activity was followed spectrophotometrically by the rate of decrease in absorbance at 265 nm. The background tautomerization rate of the substrate determined without the addition of BphH was subtracted from the former value to obtain the enzyme catalyzed rate. Assays to determine the specificity of BphH towards various HPDA substrates were carried out under

similar conditions except that the substrate concentrations were varied from 0.1 to five times K_m. Data were fitted to a Michaelis–Menten equation by nonlinear regression using the program Leonora [29]. The enzyme catalyzed rate was at least fivefold higher than the spontaneous tautomerization rates.

The pH dependence of BphH activity was performed using the three component constant ionic strength buffer containing 0.1 M Tris, 0.05 M acetic acid, and 0.05 M Mes [30]. Activity of the enzyme was tested spectrophotometrically as above over the pH range of 4.0–9.0, at 0.5 pH unit increments. Assay mixtures contain 0.35 $\mu g \cdot mL^{-1}$ BphH, 200 μM HPDA and 3 mM $MgSO_4$ in a total volume of 1 mL. The extinction coefficient of HPDA, used to calculate the specific activity, was found to be constant over the pH range and is the same as the value obtained with 100 mM potassium phosphate buffer, pH 6.0.

Determination of metal ion cofactor specificity

Purified apoenzyme (70 $\mu g \cdot mL^{-1}$) was incubated on ice for 15 min with the respective divalent metal salts at 100 mM concentrations: $MgCl_2$, $MgSO_4$, $MnCl_2$, $MnSO_4$, $CoCl_2$, $CoSO_4$, $ZnCl_2$, $ZnSO_4$ and $CaCl_2$. After incubation the samples were assayed for activity in a final volume of 1 mL containing 100 mM phosphate buffer, pH 6.0, 0.2 mM HPDA and 1 mM of the respective metal ions.

The dissociation constants for Mg^{2+} and Mn^{2+} are determined as follows. The enzyme was incubated and assayed with the respective divalent metal salts at concentrations varying from at least $0.5 \times K_d$ to $20 \times K_d$. HPDA concentration was fixed at 0.2 mM and amount of enzyme in the assay is 0.35 $\mu g \cdot mL^{-1}$. All other conditions were the same as standard activity assay. Dissociation constants (K_d) were calculated based on the Scatchard plot (V/[M] vs. V) from the equation

$$V/[M] = -V/K_d + V_{max}/K_d$$

where V is the initial velocity at various concentrations of metal ions [M], and V_{max} is the maximal catalytic rate at saturating metal ion concentration [31].

Determination of number of magnesium ions bound per enzyme subunit

Enzyme samples for analysis by atomic absorption spectroscopy were prepared according to Petrovich *et al.* [32]. Buffer and salt solutions are all prepared using metal-free water (Fisher Scientific). Briefly, 0.4 mg of enzyme was mixed with $MgSO_4$ ranging from 0 to 3 mM in a total volume of 400 μL of 20 mM sodium Hepes buffer, pH 7.5. The free and bound metal ions were separated by ultrafiltration to about 200 μL each with Amicon Microcon-30 concentrators. Saturation of Mg^{2+} in the enzyme was verified by activity assays that demonstrate the attainment of maximal HPDA transformation activity. Both the effluent and the enzyme solutions were then diluted in 20 mM sodium Hepes pH 7.5 and analyzed for Mg^{2+} content using a PerkinElmer AAnalyst800 atomic absorption spectrophotometer (Woodbridge, Ontario, Canada) operating in oxy-acetylene flame mode with a 10 cm burner head. The standard curve was generated using Mg^{2+} Atomic Absorption Standard Solution (Fisher Scientific) prepared in the same buffer as above.

Acknowledgements

This research was supported by a grant from the National Science and Engineering Research Council of Canada. S. Seah thanks the Canadian Foundation for Innovation and Ontario Innovation Trust for infrastructure support. We thank Valerie Robertson from the University of Guelph NMR centre for NMR spectra acquisition and Sean Langley for assistance with the atomic absorption spectrometer.

References

1 Focht DD (1995) Strategies for the improvement of aerobic metabolism of polychlorinated-biphenyls. *Curr Opin Biotechnol* **6**, 341–346.
2 Harayama S & Timmis KN (1990) Catabolism of aromatic hydrocarbons by *Pseudomonas*. In *Genetics of Bacterial Diversity* (Hopwood DA & Chater KF, eds), pp. 151–174. Academic Press Inc., New York.
3 Ferrandez A, Garcia JL & Diaz E (1997) Genetic characterization and expression in heterologous hosts of the 3-(3-hydroxyphenyl) propionate catabolic pathway of *Escherichia coli* K-12. *J Bacteriol* **179**, 2573–2581.
4 Seeger M, Zielinski M, Timmis KN & Hofer B (1999) Regiospecificity of dioxygenation of di- to pentachlorobiphenyls and their degradation to chlorobenzoates by the bph-encoded catabolic pathway of *Burkholderia* sp. strain LB400. *Appl Environ Microbiol* **65**, 3614–3621.
5 Lian HL & Whitman CP (1994) Stereochemical and isotopic labeling studies of 4-oxalocrotonate decarboxylase and vinylpyruvate hydratase – analysis and mechanistic implications. *J Am Chem Soc* **116**, 10403–10411.
6 Stanley TM, Johnson WH Jr, Burks EA, Whitman CP, Hwang CC & Cook PF (2000) Expression and stereochemical and isotope effect studies of active 4-oxalocrotonate decarboxylase. *Biochemistry* **39**, 718–726.
7 Pollard JR & Bugg TD (1998) Purification, characterisation and reaction mechanism of monofunctional 2-hydroxypentadienoic acid hydratase from *Escherichia coli*. *Eur J Biochem* **251**, 98–106.
8 Harayama S, Rekik M, Ngai KL & Ornston LN (1989) Physically associated enzymes produce and metabolize

2-hydroxy-2,4-dienoate, a chemically unstable intermediate formed in catechol metabolism via meta cleavage in *Pseudomonas putida*. *J Bacteriol* **171**, 6251–6258.
9 Goris J, De Vos P, Caballero-Mellado J, Park J, Falsen E Quensen JFIII,Tiedje JM & Vandamme P (2004) Classification of the biphenyl- and polychlorinated biphenyl-degrading strain LB400T and relatives as *Burkholderia xenovorans* sp. nov. *Int J Syst Evol Microbiol* **54**, 1677–1681.
10 Hofer B, Backhaus S & Timmis KN (1994) The biphenyl/polychlorinated biphenyl-degradation locus (bph) of *Pseudomonas* sp. LB400 encodes four additional metabolic enzymes. *Gene* **144**, 9–16.
11 Studier FW & Moffatt BA (1986) Use of bacteriophage T7 RNA polymerase to direct selective high-level expression of cloned genes. *J Mol Biol* **189**, 113–130.
12 Dente L & Cortese R (1987) pEMBL: a new family of single-stranded plasmids for sequencing DNA. *Methods Enzymol* **155**, 111–119.
13 de Lorenzo V, Eltis L, Kessler B & Timmis KN (1993) Analysis of *Pseudomonas* gene products using lacIq/Ptrp-lac plasmids and transposons that confer conditional phenotypes. *Gene* **123**, 17–24.
14 Cowan JA (1997) *Inorganic Biochemistry: an Introduction*, 2nd edn. John Wiley and Sons, Inc., New York.
15 Wasserfallen A (1989) *Etude Biochemique et Genetique de la specificite de al catechol 2,3-dioxygenase de* Pseudomonas putida. PhD Thesis. University of Geneva, Geneva, Switzerland.
16 Menn FM, Zylstra GJ & Gibson DT (1991) Location and sequence of the *todF* gene encoding 2-hydroxy-6-oxohepta-2,4-dienoate hydrolase in *Pseudomonas putida* F1. *Gene* **104**, 91–94.
17 Shannon RD (1976) Revised effective ionic radii and systematic studies of interatomic distances in halides and chalcogenics. *Acta Crystallogr Section A* **32**, 751–767.
18 Barriault D, Vedadi M, Powlowski J & Sylvestre M (1999) *cis*-2,3-Dihydro-2,3-dihydroxybiphenyl dehydrogenase and cis-1, 2-dihydro-1,2-dihydroxynaphathalene dehydrogenase catalyze dehydrogenation of the same range of substrates. *Biochem Biophys Res Commun* **260**, 181–187.
19 Seah SY, Labbe G, Nerdinger S, Johnson MR, Snieckus V & Eltis LD (2000) Identification of a serine hydrolase as a key determinant in the microbial degradation of polychlorinated biphenyls. *J Biol Chem* **275**, 15701–15708.
20 Vaillancourt FH, Haro MA, Drouin NM, Karim Z, Maaroufi H & Eltis LD (2003) Characterization of extradiol dioxygenases from a polychlorinated biphenyl-degrading strain that possess higher specificities for chlorinated metabolites. *J Bacteriol* **185**, 1253–1260.
21 Hanahan D (1983) Studies on transformation of *Escherichia coli* with plasmids. *J Mol Biol* **166**, 557–580.
22 Tabor S & Richardson CC (1985) A bacteriophage T7 RNA polymerase/promoter system for controlled exclusive expression of specific genes. *Proc Natl Acad Sci USA* **82**, 1074–1078.
23 Herrero ML, V & Timmis KN (1990) Transposon vectors containing non-antibiotic resistance selection markers for cloning and stable chromosomal insertion of foreign genes in Gram-negative bacteria. *J Bacteriol* **172**, 6557–6567.
24 Sambrook J, Fritsch EF & Maniatis T (1989) *Molecular Cloning: A Laboratory Manual*. Cold Spring Harbour Laboratory Press, Cold Spring Harbour, New York.
25 Seah SY, Terracina G, Bolin JT, Riebel P, Snieckus V & Eltis LD (1998) Purification and preliminary characterization of a serine hydrolase involved in the microbial degradation of polychlorinated biphenyls. *J Biol Chem* **273**, 22943–22949.
26 Pollard JR, Henderson IMJ & Bugg TDH (1997) Chemical and biochemical properties of 2-hydroxypentadienoic acid, a homologue of enolpyruvic acid. *Chem Commun* **19**, 1885–1886.
27 Bradford MM (1976) A rapid and sensitive method for the quantitation of microgram quantities of protein utilizing the principle of protein-dye binding. *Anal Biochem* **72**, 248–254.
28 Laemmli UK (1970) Cleavage of structural proteins during the assembly of the head of bacteriophage T4. *Nature* **227**, 680–685.
29 Cornish-Bowden A (1995) *Analysis of Enzyme Kinetic Data*. Oxford University Press, New York.
30 Ellis KJ & Morrison JF (1982) Buffers of constant ionic strength for studying pH-dependent processes. *Methods Enzymol* **87**, 405–426.
31 Newman JW, Morisseau C, Harris TR & Hammock BD (2003) The soluble epoxide hydrolase encoded by EPXH2 is a bifunctional enzyme with novel lipid phosphate phosphatase activity. *Proc Natl Acad Sci USA* **100**, 1558–1563.
32 Petrovich RM, Litwin S & Jaffe EK (1996) Bradyrhizobium japonicum porphobilinogen synthase uses two Mg(II) and monovalent cations. *J Biol Chem* **271**, 8692–8699.